Stereochemical Investigation of Palladium(II) Complexes with Phenanthroline Ligands: A Molecular Mechanics Approach

Mario Calligaris,[a] Ennio Zangrando,*[a] and Barbara Milani,[a] Angelica Marson[a,‡]

Keywords: Stereochemistry / Molecular mechanics / Copolymerisation / Phenanthroline / Palladium

Specific force field parameters have been derived through an optimisation procedure based on crystal structure data to describe the geometry of Pd^{II}-phenanthroline complexes. The X-ray structure of $[Pd(CH_3)(3\text{-}s\text{Bu-phen})_2][OTf]$ is also reported. Molecular mechanics calculations show that intramolecular steric interactions yield severe distortions from a square-planar geometry of the metal atom, both in bischelated $[Pd(3\text{-R-phen})_2]^{2+}$ and monochelated $[Pd(CH_3)(3\text{-R-phen})_2]^+$ complexes. A complete stereochemical analysis of the possible diastereoisomers of this last complex (R = *s*Bu) allows the rationalisation of its fluxional behaviour observed in solution. Complexes like $[Pd(H)(3\text{-tmp-phen})_2]^+$ and $[Pd\{CH(C_6H_5)CH_2C(O)OCH_3\}(3\text{-tmp-phen})(CH_3OH)]^+$ (tmp = 1,2,2-trimethylpropyl) have also been investigated as species reasonably involved in the copolymerisation reactions. It is suggested that the remarkable increase of the copolymer molecular weight obtained with the 3-tmp-phen ligand derives from the steric destabilisation of an intermediate species postulated for the termination reaction.

(© Wiley-VCH Verlag GmbH & Co. KGaA, 69451 Weinheim, Germany, 2005)

Introduction

Bischelated palladium(II) compounds with bidentate nitrogen-donor ligands, such as 1,10-phenanthroline (phen) and its derivatives, have been shown to act as efficient precatalysts in the CO/styrene copolymerisation reaction.[1–3] Some stereochemical aspects of these complexes have been investigated both in solution and in the solid state, providing some information about the conformational flexibility of the bischelated $[Pd(phen)_2]^{2+}$ complex,[1,4] and the fluxional behaviour of the monocationic derivatives, $[Pd(R)(phen)_2]^+$ (R = CH_3,[5] and CH_2NO_2[6]), where one phen ligand is monocoordinated.

In order to rationalise the observed structural properties of this kind of complexes, a thorough molecular mechanics (MM) investigation has been undertaken, on the basis of a specific force field. The force field parameters have been derived from the available crystal data for $[Pd(phen)_2][OTf]_2$ (**1**),[7] $[Pd(3\text{-}i\text{Pr-phen})_2][PF_6]_2$ (**2**),[8] $[Pd(3\text{-}n\text{Bu-phen})_2][PF_6]_2$ (**3**),[8] and $[Pd(CH_3)(phen)_2][PF_6]$ (**4**),[5] besides those presented in this paper for $[Pd(CH_3)(3\text{-}s\text{Bu-phen})_2][PF_6]$ (**5**) (OTf = triflate, 3-*i*Pr-phen = 3-isopropyl-phenanthroline, 3-*n*Bu-phen = 3-normal-butyl-phenanthroline, 3-*s*Bu-phen = 3-secondary-butyl-phenanthroline). The crystal structure of the latter has been determined in order to examine the influence of a bulky group in position 3 of phen on the overall geometry of the organometallic cation.

The MM study has been extended to the diastereoisomers of the hydride complex, $[Pd(H)(phen)_2]^+$, and of its 3-(1,2,2-trimethylpropyl) derivative, $[Pd(H)(3\text{-tmp-phen})_2]^+$, in order to get some insight into the structure of species proposed to be present in the catalytic copolymerisation process.[1,2] The 3-tmp group has been considered in view of the significant increase of both productivity and polymer molecular weight obtained after introduction of this side group in the phen ligand.[3] Furthermore, models of the copolymer chain-initiating species, like $[Pd\{CH(C_6H_5)CH_2C(O)OCH_3\}(N\text{–}N)(CH_3OH)]^+$, have also been investigated with N–N = phen and 3-tmp-phen with the aim of elucidating the role of the side group in the chain growth process.

Results and Discussion

Force Field

The molecular strain energy, *E*, has been calculated according to the AMBER force field,[9] as the sum of the harmonic deformation functions for bond lengths (d), bond angles (θ), torsion angles (including improper-torsion angles, which model out-of-plane displacements) (ψ), and the van der Waals and electrostatic energy contributions [Equation (1)].

[a] Department of Chemical Sciences, University of Trieste, Via L. Giorgieri 1, 34127 Trieste, Italy
Fax: +39-040-558-3903
E-mail: zangrando@univ.trieste.it
[‡] Current address: Institute of Molecular Chemistry, Homogeneous Catalysis, University of Amsterdam, Nieuwe Achtergracht 166, 1018 WV Amsterdam, The Netherlands

Supporting information for this article is available on the WWW under http://www.eurjic.org or from the author.

$$E = \Sigma_b[k_b(d - d°)^2] + \Sigma_a[k^\theta(\theta - \theta°)^2] + \Sigma_t\{\tfrac{1}{2}V_n[1 + \cos(n \cdot \psi - \psi°)]\} + \Sigma_{ij}[(a_{ij}/r_{ij}^{12}) - (b_{ij}/r_{ij}^{6}) + (q_i \cdot q_j/D \cdot r_{ij})] \quad (1)$$

Summations in (1) are extended over all bonds, angles, torsions and pairs of non-bonded atoms *i*–*j*, separated by the distance r_{ij} . In the last summation, $a_{ij} = (\varepsilon_i\varepsilon_j)^{1/2}(r_i* + r_j*)^{12}$, $b_{ij} = 2(\varepsilon_i\varepsilon_j)^{1/2}(r_i* + r_j*)^6$, where r_i* is the van der Waals radius of atom type *i*, and ε_i is the well depth for two atoms of type *i*; q_i and q_j are the atomic charges and *D* is the dielectric constant, here treated as a distance-dependent variable ($D = r_{ij}$). Electrostatic and nonbonded atom interactions have both been reduced by a scale factor of 0.5 when atoms are only separated by three bonds. In all calculations, the trigonal carbon and nitrogen atoms have been treated using the improper torsion parameters of aromatic carbon atoms given in AMBER.[9] As in previous computations,[10,11] torsion barriers around the coordination bonds have been fixed to zero.

Energy calculations have been performed with a Pentium III PC, using the HyperChem. 6.01 molecular modelling system.[12] The Polak–Ribiere version of the conjugate gradient method has been used in all energy minimisation calculations with a convergence criterion of 0.001 kcal mol^{-1} Å^{-1} (1 kcal = 4.184 kJ). Atomic charges have been calculated by the semi-empirical ZINDO/1 method, suitable for the molecular orbital calculations of second-row transition metal complexes.[12] A local program has been used for all the geometrical calculations.[13]

Because phenanthroline and palladium atom types were not available in AMBER, the force field has been implemented with the addition of the new atom types (Figure SA in the Supporting Information) and the relative force field constants (Tables SA and SB in the Supporting Information). The "stretching" potential constants (k^d) for the *i*–*j* bonds have been calculated according to the Badger's rule,[14] $k^d_{ij} = 71.94 \cdot [(A_{ij} - D_{ij})/(d°_{ij} - D_{ij})]^3$ kcal mol^{-1} Å^{-2}, using the A_{ij} and D_{ij} parameters proposed by Herschbach and Laurie.[15] The $d°$ values for the phenanthroline C–N and C–C bonds have been derived from the mean values, calculated from the accurate crystal structure data of complexes **1–3**, while the $d°$ values for the Pd–N and Pd–C bonds (Table SA), together with the ε_{Pd} (0.693 kcal mol^{-1}) and $r*_{Pd}$ (1.928 Å) van der Waals parameters, have been optimised according to the Simplex-method procedure, already used for the derivation of force field constants in ruthenium(II)[10] and cobalt(III) [11] metal complexes. The minimised function is GOF = $[\Sigma_i w_i\Delta_i^2/(n_{obs} - n_p)]^{1/2}$, where the summation is extended to all the differences, Δ_i , between each observed and calculated value of the n_{obs} data (522 in the present case); w_i is the weight ($1/\sigma_i^2$) of each observation, and n_p is the total number of variable parameters (7, in the present case). The "bending" constants (k^θ) for the *i*–*j*–*k* bond angles have been calculated according to the Halgren's equation:[16] $k^\theta_{ijk} = 125.9 \cdot \{Z_iC_jZ_k(d°_{ij} + d°_{ik})^{-1}(\theta°_{ijk})^{-2}\exp[-2(d°_{ij} - d°_{jk})^2/(d°_{ij} + d°_{ik})^2]\}$ kcal mol^{-1} rad^{-2}.

The values of the *C* and *Z* parameters for palladium (1.3267 and 3.2039, respectively) have been obtained by the optimisation procedure described above, whereas for the carbon, nitrogen and hydrogen atoms, the Halgren's values have been used. No restraint has been included in the energy minimisation during the force field parameter optimisation procedure.

Because of the lack of suitable experimental structural data, the stretching (Table SA) and bending (Table SB) force constants of the Pd–H and Pd–O bonds have been simply calculated by the Badger's and Halgren's equations, assuming $d°$(Pd–H) = 1.6 Å, and $d°$(Pd–O) = 2.01 Å.

Minimum energy structures have been found by the Conformational Search routine of HyperChem[12] and the conformational analysis has been carried out with local Excel© Macro functions that allow the minimisation of the strain energy as the conformation of the cation is varied through rotation around the Pd–N bond of the monocoordinated phen ligand.

As shown in Table 1, the agreement between observed and calculated bond lengths and angles for the five complexes, **1–5**, used for the optimisation of the force field parameters, is quite satisfactory, specially after imposing a restraint on the Pd···N(apical) distance in the methyl derivatives **4** and **5** (see below). In fact, the average differences, $<\Delta>$, between observed and calculated values, are low enough to show the absence of large systematic errors, and the weighted root-mean-square deviations (wrms = $[(\Sigma_i w_i\Delta_i^2)/\Sigma_i w_i]^{1/2}$) are lower than the mean ranges of chemically equivalent structural parameters, observable in the crystal structures of **1–3** (e.g. 0.022, 0.018, and 0.023 Å for the Pd–N, N–C, and C–C bond lengths).

Table 1. Average differences $<\Delta>$ between observed and calculated bond lengths and angles, weighted root-mean-square values (wrms), and number of observations (*n*) used in the force field parameter optimisation procedure for structures **1–5**. X, Y and Z represent carbon and nitrogen atoms.

Distances [Å]	$<\Delta>$[a]	$<\Delta>$[b]	wrms[a]	wrms[b]	*n*
Pd–X	–0.010	–0.008	0.016	0.015	20
X–Y	0.001	0.001	0.016	0.016	182
Angles [°]	$<\Delta>$[a]	$<\Delta>$[b]	wrms[a]	wrms[b]	*n*
X–Pd–Y	–0.4	–0.3	2.0	1.9	30
Pd–X–Y	0.6	0.6	1.0	0.9	36
X–Y–Z	0.3	0.3	1.4	1.3	252

[a] No restraint. [b] Pd···N distance restrained to 2.730 Å with a force constant of 1000 kcal mol^{-1}.

Moreover, the overall shape of the minimised structures of the cations, $[Pd(phen)_2]^{2+}$ (**1**) and $[Pd(3\text{-R-phen})_2]^{2+}$ (R = *i*Pr for **2** and *n*Bu for **3**), is reasonably close to that found in the crystal structures (Table 2), the differences being attributable to the different packing environments.

The consistency of the force field is further illustrated by its ability to reproduce, in the methyl derivatives **4** and **5**, the increase of the Pd–N bond lengths on going from the chelate to the monocoordinated ligand, and the increase of the Pd–N bond length *trans* to the methyl group (Table 3). The deformation of the Pd–N–C bond angles in the monocoordinated phenanthroline ligand is also well reproduced, as well as the orientation of the ligands, shown by the tor-

 © 2005 Wiley-VCH Verlag GmbH & Co. KGaA, Weinheim

Table 2. Experimental and calculated (*italic*) conformational parameters for $[Pd(phen)_2]^{2+}$ and $[Pd(3\text{-R-phen})_2]^{2+}$ (R = *i*Pr, *n*Bu) complexes.

Complex	α[a]	β[a,b]	γ[a,b]
twist conformation:			
$[Pd(phen)_2][ClO_4]_2$[c]	18.7	2.9	3.0
$[Pd(phen)_2][OTf]_2$[d]	21.4	2.0, 5.6	5.2, 3.1
$[Pd(phen)_2][BF_4]_2$[e,f]	24.7	0.4	1
	20.1	0.0, 0.6	1, 3
$[Pd(phen)_2]^{2+}$[g]	*17.7*	*0.2, 0.2*	*0.7, 0.8*
$[Pd(3\text{-}i\text{Pr-phen})_2][PF_6]_2$[h]	18.8	7.4	5.0
$[Pd(3\text{-}i\text{Pr-phen})_2]^{2+}$[g]	*16.9*	*0.3*	*0.7*
$[Pd(3\text{-}n\text{Bu-phen})_2][PF_6]_2$[h]	23.2	3.6	3.4
$[Pd(3\text{-}n\text{Bu-phen})_2]^{2+}$[g]	*17.0*	*0.2*	*0.7*
bow-step conformation:			
$[Pd(phen)_2][PF_6]_2$[i]	0.0	16.2	13.4
$[Pd(phen)_2]^{2+}$[g]	*0.0*	*9.2, 9.3*	*13.4*

[a] See caption of Figure 1 for angle definitions. [b] One value for symmetry related phen moieties. [c] Ref.[17] [d] Ref.[7] [e] Ref.[1] [f] Two crystallographically independent molecules. [g] Minimum strain energy structure. [h] Ref.[8] [i] Ref.[4]

sion angle ψ and the dihedral angle τ (see footnotes h and i in Table 3). Data in Table 3 show the remarkable improvement in the structural data after inclusion of the restraint in the Pd···N distance, introduced to account for a possible weak covalent bonding interaction between Pd and the apical N atom (see below).

Table 3. Selected observed and calculated parameters in the $[Pd(CH_3)(phen)_2]^+$ (**4**), and $[Pd(CH_3)(3\text{-}s\text{Bu-phen})_2]^+$ (**5**) complexes; labels from Figure 2 apply to both complexes.

	Obs.[a]	Calcd.[a,b]	Calcd.[a,c]
Pd–C(13) [Å]	2.018(9), 2.010(10)	2.006, 2.006	2.007, 2.006
Pd–N(1) [Å][d]	2.036(8), 2.030(8)	2.053, 2.053	2.052, 2.052
Pd–N(2) [Å][f]	2.115(8), 2.122(8)	2.121, 2.121	2.119, 2.120
Pd–N(3) [Å][e]	2.040(8), 2.065(7)	2.097, 2.097	2.086, 2.086
Pd···N(4) [Å]	2.737(8), 2.716(7)	2.983, 2.987	2.752, 2.752
Pd–N(1)–C(1) [°][d]	129.1(6), 128.2(6)	127.3, 127.4	127.4, 127.6
Pd–N(3)–C(14) [°][e]	116.2(6), 116.6(7)	113.6, 113.7	116.5, 116.7
d [Å][g]	0.075, 0.062	–0.006, –0.004	0.047, 0.055
ψ [°][h]	90.5, 103.1	106.9, 110.2	99.2, 105.3
τ [°][i]	89.4, 75.5	73.7, 69.4	80.9, 73.6

[a] The first value refers to phen, the second one to 3-*s*Bu-phen. [b] Calculated values without restraints. [c] Calculated values with the Pd···N(4) distance restrained to 2.730 Å. [d] Chelate ligand. [e] Monocoordinated ligand. [f] *trans* to CH_3. [g] Metal atom displacement from the basal CN_3 plane towards the apical N atom. [h] Torsion angle N(2)–Pd–N(3)–C(14). [i] Dihedral angle between the phen (N_2C_{14}) mean planes.

Molecular and Crystal Structures

$[Pd(phen)_2]^{2+}$ and $[Pd(3\text{-R-phen})_2]^{2+}$ Complexes

Previous structural investigations of $[Pd(phen)_2]^{2+}$ complexes showed that the cations are characterised by significant ligand distortions due to the steric repulsion between the α-hydrogen atoms.[1,4,7,17] In most cases, the steric crowding is relieved by a tetrahedral distortion of the PdN_4 core yielding a *twist* conformation, in which the dihedral angle, α, between the PdN_2 planes (π_1 and π_1' in Figure 1) ranges from 18° to 25°, depending upon the nature of the anion (Table 2).[1,7,17] A similar conformation has also been found in the phenanthroline-substituted cations $[Pd(3\text{-R-phen})_2]^{2+}$ (α = 18.8 and 23.2°, for R = *i*Pr and *n*Bu, respectively),[8] and in the platinum(II) complex $[Pt(phen)_2][Cl]_2\cdot 3H_2O$ (α = 20.9°).[18] On the other hand, in the case of $[Pd(phen)_2][PF_6]_2$, the repulsive interactions are partly alleviated by a bending on opposite sides of the π_1, π_2 and π_1', π_2' planes (dihedral angles β, β') giving rise to a *step* geometry (α = 0°, $\beta = \beta'$ = 16.2°), with the five-membered rings in an *envelope* conformation.[4] This deformation is accompanied by a tilting, towards the same side, of the π_3, π_4 planes (dihedral angle γ = 13.4°) so that each phen ligand exhibits a *bow* conformation, and the cation acquires an overall *bow-step* shape.[4] However, inspection of Table 2 shows that also in the *twist* conformations there can be some "s*tepping*" and "*bowing*", like in $[Pd(3\text{-}i\text{Pr-phen})_2][PF_6]_2$ (β = 7.4° and γ = 5.0°) and in $[Pd(phen)_2][OTf]_2$, where, for one ligand, β = 5.6° and γ = 5.2°. Interestingly, in $[Pd(phen)_2][BF_4]_2$,[1] β and γ are much smaller, probably because of weaker intermolecular interactions, due to the lack of any Pd···O or Pd···F coordinating interaction, present in the other compounds.[7,17] This is in agreement with the observation that the β and γ values found in the BF_4 compound are close to those calculated for the three isolated cations, $[Pd(phen)_2]^{2+}$, $[Pd(3\text{-}i\text{Pr-phen})_2]^{2+}$ and $[Pd(3\text{-}n\text{Bu-phen})_2]^{2+}$ (Table 2), in the absence of any packing effect.

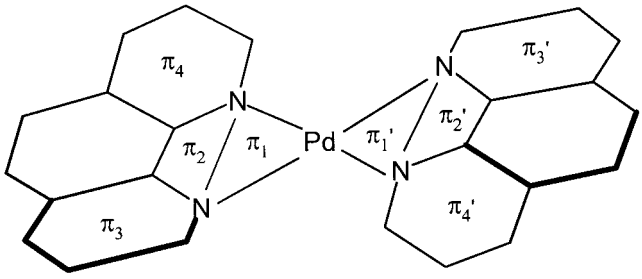

Figure 1. Planes (π_i) used to describe the conformation of the $[Pd(phen)_2]^{2+}$ complex; the dihedral angle α, between π_1 and π_1', defines the "twisting" of the two ligands, β (β'), between π_1, π_2 (π_1', π_2'), defines the "step", and γ (γ'), between π_3, π_4 (π_3', π_4'), defines the "bow".

The present MM calculations show that the $[Pd(phen)_2]^{2+}$ cation in the *twist* conformation exhibits a total strain energy about 3.7 kcal mol^{-1} lower than that in the *bow-step* conformation, mainly because of a lower torsional energy contribution. This indicates that the *bow-step* conformation is only slightly less stable, confirming the hypothesis that, in the solid state, it can be stabilised by van der Waals and electrostatic forces, without the need for particular stacking interactions.[1]

 © 2005 Wiley-VCH Verlag GmbH & Co. KGaA, Weinheim

It is interesting to observe that the *twist* distortion gives a two-bladed propeller shape to the $[Pd(phen)_2]^{2+}$ cation (C_2 point group symmetry), whose chirality can be assigned using the Δ, Λ descriptors.[19] On the contrary, the *bow-step* conformation is achiral being characterised by a C_{2v} symmetry.

Finally, it is worth noting that, in the solid state, the $[Pd(3\text{-}i\text{Pr-phen})_2]^{2+}$ and $[Pd(3\text{-}n\text{Bu-phen})_2]^{2+}$ complexes, have the side groups placed on the same side, in a *syn* geometry. In fact, MM calculations show that this isomer, for both of the isolated cations, exhibits a strain energy slightly lower than that of the *anti* isomer (*i*Pr, 0.8 kcal mol^{-1}; *n*Bu, 1.1 kcal mol^{-1}). This is qualitatively in agreement with the results of a DFT study performed on the same derivatives.[8] However, the energy differences are rather low, suggesting that the stabilisation of the *syn* isomers in the solid state is probably due to packing effects.

$[Pd(CH_3)(phen)_2]^+$ and $([Pd(CH_3)(3\text{-R-phen})_2]^+$ Complexes

The most interesting structural feature in the crystals of the $[Pd(CH_3)(phen)_2]^+$,[5] and $[Pd(CH_3)(3\text{-}s\text{Bu-phen})_2]^+$ (Figure 2) cations is the distorted square-planar geometry of the Pd atoms with one phenanthroline molecule acting as a monocoordinated ligand. The orientation of this phen group is such that the uncoordinated nitrogen atom, through rotation around the Pd–N bond, occupies a pseudo-apical position at 2.73(1) Å from the metal atom. The rotation around the Pd–N bond is measured by the torsion angle ψ (N[2]–Pd–N(3)–C(14) in Figure 2), which is 90.5° and 103.0° in $[Pd(CH_3)(phen)_2]^+$[5] and $[Pd(CH_3)(3\text{-}s\text{Bu-phen})_2]^+$, respectively (Table 3). The two phenanthroline ligands are nearly perpendicular to each other in the phen complex (dihedral angle τ = 89.4°);they form a narrower angle in the 3-*s*Bu-phen derivative (τ = 75.5°). A similar structure has been found in the related complex $[Pd(CH_2NO_2)(phen)_2][PF_6]$, where the Pd···N distance is 2.674(3) Å and τ = 88.9°.[6]

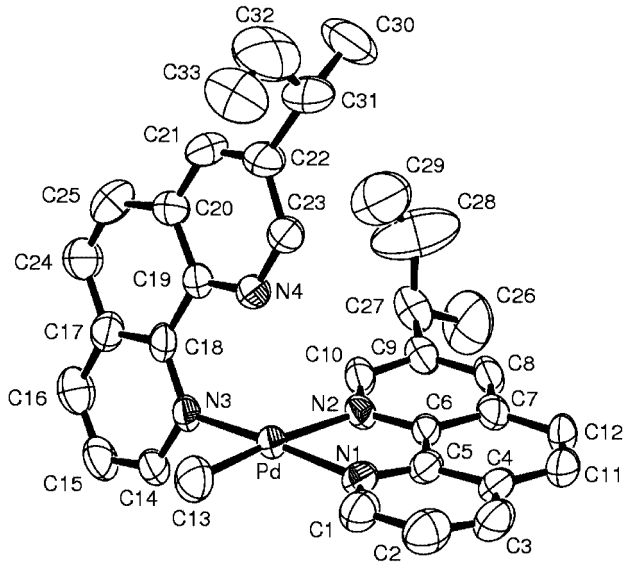

Figure 2. ORTEP drawing of the $[Pd(CH_3)(3\text{-}s\text{Bu-phen})_2]^+$ cation (thermal ellipsoids at 40% probability level).

The strain energy minimisation (without any restraint), starting from the crystal structure coordinates of $[Pd(CH_3)(phen)_2]^+$, yields for the calculated structures ψ = 106.9° and τ = 73.7°, and, in the case of $[Pd(CH_3)(3\text{-}s\text{Bu-phen})_2]^+$, ψ = 110.2° and τ = 69.4°, not too far from the solid-state values. This indicates that the orientation of the monocoordinated ligand is essentially determined by intramolecular van der Waals and electrostatic interactions. On the other hand, in the minimum-strain-energy structures, the average Pd···N distance is 2.985(1) Å. Interestingly, this distance is significantly shorter than the sum of the assumed van der Waals radii (1.93+1.82 = 3.75 Å), but much longer than the experimental distances, which suggests the presence of some Pd–N valence-bonding interaction not modelled in the present force field (no specific d^o and k^b values). In this respect, we must observe that the van der Waals radius of 1.93 Å, derived for Pd^{II} in the present force field, in correspondence with ε_{Pd} = 0.69 kcal mol^{-1}, is somewhat intermediate between the previously proposed values of 1.65 Å[20] and 2.60 Å,[21] and not far from 1.7 Å (ε_{Pd} = 0.2 kcal mol^{-1}) reported by Hambley, from MM modelling of nonbonded Pd···H and Pd···S interactions.[22] In fact, this last value might be an underestimate in the case of weakly attractive (agostic) interactions with the metal atom.[22]

The presence of a bonding contribution is further indicated by the displacement of the palladium atom from the coordination mean plane (Table 3). In fact, by restraining the Pd···N distance to 2.730 Å a remarkable improvement of the Pd out-of-plane distance is obtained, as well as of ψ and τ (Table 3). On the basis of these results, we can assume that the palladium coordination polyhedron is intermediate between a square-planar and a square-pyramidal geometry, even though, in this last case, a Pd–N distance of about 2.347 Å should be expected for an apical bond.[23] However, a constraint on such a value for the Pd···N distance causes a dramatic increase of the strain energy (≈ 75 kcal mol^{-1}), essentially because of the increase of the van der Waals energy term. Thus, the attractive bonding interaction between the Pd and N atoms seems to be in balance with significant intraligand repulsive forces.

^{1}H NMR spectroscopy has shown the equivalence, in solution, of the two phen ligands, indicating the presence of a dynamic process, which involves either the exchange between the unbound nitrogen atom of the monocoordinated ligand and that of the chelate ligand *trans* to the methyl group (*opening-closure*), or the exchange of the two nitrogen atoms at the same coordinating site (*flipping*).[5]

In order to investigate the steric aspects of this process, we have undertaken an analysis of the strain energies of the species possibly involved. From a structural point of view, we have only one stereoisomer in the case of the phen ligand ($[Pd(CH_3)(phen)_2]^+$) and four distinct diastereoisomers in the case of the 3-alkyl-phen ligands ($[Pd(CH_3)(3\text{-R-phen})_2]^+$, with R = *i*Pr and *s*Bu), depending on the relative position of the substituents (Figure 3).

 © 2005 Wiley-VCH Verlag GmbH & Co. KGaA, Weinheim

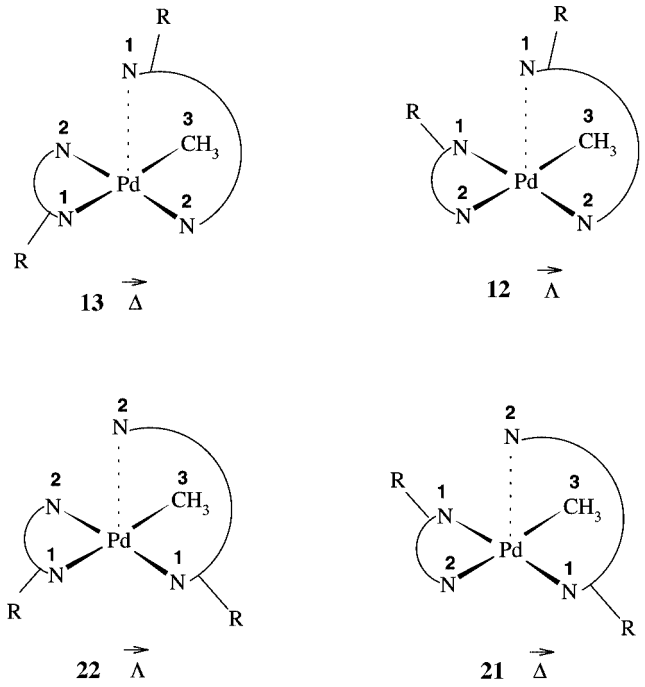

Figure 3. Sketch of the stereoisomers of the $[Pd(CH_3)(3\text{-R-phen})_2]^+$ cations, with their stereochemical descriptors; ranking numbers are also reported.

The different diastereoisomers are identified by a two-digit configuration index formally assuming a bischelated complex with a square pyramidal geometry.[19] For the 3-R-phen complexes, the priority of the ligating atoms decreases in the order N(–R) > N > C, with ranking numbers 1, 2 and 3, respectively (Figure 3). The chirality of these complexes (C_1 symmetry) can be conveniently described by the "oriented-skew-lines" reference system, considering the N···N lines of the 3-R-phen ligands oriented from N(–R) to N.[24]

It is to be noted that the change of the apical position implies an inversion of the complex configuration, with inversion of the sign of ψ. Furthermore, because of the approximate coplanarity of the atoms in the phenanthroline ligands and in the coordination basal plane, the variation of ψ implies a variation of the dihedral angle τ such that $|\psi| + \tau \approx 180°$ (Table 4). Therefore, the rotation of the phen ligand around the Pd···N axis corresponds to the swinging of the ligand plane around the Pd···N "hinge".

In order to investigate the isomer stability, we have calculated the strain energy for the four diastereoisomers of $[Pd(CH_3)(3\text{-}s\text{Bu-phen})_2]^+$, with different combinations of the *R*/*S* chirality of the *s*Bu groups (Table 4). ΔE and ψ (configuration $\vec{\Delta}$) values have been calculated with and without the restraint on the Pd···N distance. However, inspection of Table 4 shows that there are small energy differences between the two cases. It is worthy of note that after introduction of the restraint, the lowest energy is exhibited by isomer **13**, in which the asymmetric carbon atoms of the *sec*-butyl group in the chelated and that in the monocoordinated phen ligands have opposite configurations, as in the diastereoisomers **13** (*R*–*S*) and **13** (*S*–*R*). In fact, the former isomer has been found in the crystal. This shows once again that the introduction of the Pd···N restraint is necessary for the best description of the structural properties of these complexes. As shown in Table 4, in each diastereoisomer, ΔE is nearly unaffected by the chirality of the *s*Bu groups, while it increases slightly, in the order **13** < **22** < **21** < **12**, with a maximum energy difference of about 1.3 kcal mol^{-1}. Finally, calculations show that changes in the conformation of the *s*Bu groups (φ angles) cause small changes in ΔE.

Table 4. Scaled strain energies [kcal mol^{-1}] for the four diastereoisomers of $[Pd(CH_3)(3\text{-}s\text{Bu-phen})_2]^+$, all in configuration $\vec{\Delta}$ considering the possible combinations of the ligand chirality; ΔE represents the strain energy differences with respect to the lowest-energy isomer; some conformational parameters (see Figure 2 for labels) are also reported for the "restrained" structures.

Isomer	Chirality[a]	ΔE[b]	ΔE[c]	Ψ [°][d]	τ [°][e]	φ_1 [°][f]	φ_2 [°][g]	φ_1' [°][h]	φ_2' [°][i]
13	*R*–*S*	0.6	0.0	101.7	79.0	117.7	–53.6	60.8	54.8
	S–*R*	0.2	0.0	101.7	79.0	60.6	54.5	117.9	–54.3
	S–*S*	0.0	0.1	107.5	71.7	57.5	52.1	118.2	54.9
	R–*R*	0.3	0.3	106.1	73.8	–60.4	–54.2	117.1	–53.9
22	*S*–*S*	0.4	0.4	–103.3	77.5	58.8	52.5	59.0	52.4
	S–*R*	0.5	0.6	–78.7	101.6	58.1	53.2	–59.8	–53.5
	R–*S*	0.6	0.6	–103.6	76.7	–59.1	–53.5	59.7	53.1
	R–*R*	0.8	0.8	–103.3	77.0	–59.1	–53.6	116.5	–53.5
21	*S*–*S*	1.1	1.1	103.7	76.8	60.1	54.4	59.4	53.9
	S–*R*	1.2	1.1	103.4	77.2	60.1	54.4	–60.3	–54.3
	R–*S*	1.1	1.1	103.6	76.9	–60.0	–54.3	59.5	54.0
	R–*R*	1.2	1.1	103.4	77.2	–60.0	–54.3	–54.3	–54.3
12	*S*–*S*	1.4	1.3	–80.2	100.5	59.2	53.7	59.6	54.3
	S–*R*	1.4	1.3	–102.7	77.6	59.7	54.0	–60.3	–54.7
	R–*S*	1.4	1.3	–102.7	77.9	–60.1	–54.4	60.3	54.8
	R–*R*	1.4	1.3	–81.6	98.8	–60.2	–54.5	–60.4	–54.8

[a] The configuration of the asymmetric carbon atoms refers to the *s*Bu group in the chelate and in the monocoordinated ligand, respectively. [b] No restraint on the Pd···N distance, which averages 2.987(3) Å. [c] Pd···N distance restrained to 2.752 Å. d N(2)–Pd–N(3)–C(14). [e] Footnote i in Table 3. [f] C(10)–C(9)–C(27)–C(28). [g] C(9)–C(27)–C(28)–C(29). [h] C(23)–C(22)–C(31)–C(32). [i] C(22)–C(31)–C(32)–C(33).

 © 2005 Wiley-VCH Verlag GmbH & Co. KGaA, Weinheim

As shown in Table 4, the minimum energy structures are provided by *gauche*-like conformations ($\varphi \approx \pm 60°, \pm 120°$).

The possibility of rotation of the monocoordinated phen ligand around its Pd–N bond (torsion angle ψ) has been investigated through a conformational analysis of the $[Pd(CH_3)(phen)_2]^+$ and $[Pd(CH_3)(3\text{-}s\text{Bu-phen})_2]^+$ cations, imposing the Pd···N restraint, and considering the enantiomeric species with $\psi > 0$, in the range between 50° and 130°.

As shown in Figure 4, in the case of the phen complex, "free" rotation is limited to a ψ range between 65° and 115°, in correspondence of the broad low-energy region ($\Delta E < 1$ kcal mol^{-1}), with two minima around $\psi = 80°$ and $\psi = 100°$, the second one with an energy only 0.2 kcal mol^{-1} higher. A similar behaviour is found for the **22** $\vec{\Delta}$ (*R*–*S*) isomer of the 3-*s*Bu-phen derivative ($\Delta E = 0.3$ kcal mol^{-1}), whereas its other *R*–*S* diastereoisomers, as well as all those of the **12** and **21** isomers, exhibit the opposite trend, having the deepest minimum at $\psi \approx 100°$–$105°$, with ΔE values varying from 0.1 to 0.3 kcal mol^{-1}. Calculations show that in the case of isomer **13** $\vec{\Delta}$, the energy at $\psi \approx 80°$ slightly increases in the order (*R*–*R*) < (*S*–*S*) < (*S*–*R*) < (*R*–*S*), with ΔE in the range 0.4–0.6 kcal mol^{-1}.

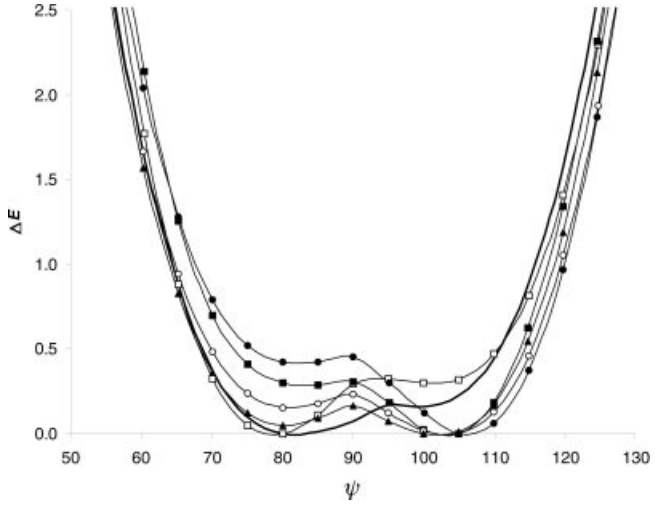

Figure 4. Plot of ΔE [kcal mol^{-1}] vs. the rotation angle ψ [°] (Pd···N restraint) for $[Pd(CH_3)(phen)_2]^+$ (thick line), and for some isomers of $[Pd(CH_3)(3\text{-}s\text{Bu-phen})_2]^+$: **22** $\vec{\Lambda}$ (*R*–*S*) (□), **22** $\vec{\Lambda}$ (*R*–*R*) (■), **12** $\vec{\Lambda}$ (*R*–*R*) (#9650;), **21** $\vec{\Delta}$ (*R*–*R*) (○), and **13** $\vec{\Delta}$ (*R*–*R*) (●).

The small differences calculated for the strain energies (Table 4) account for the fluxional behaviour in solution of this kind of complexes, and the proposed ligand exchange mechanism.[5] In fact, the *flipping* process yields the equilibration between isomers **13** and **22** ($E_{22} - E_{13} \approx 0.4$ kcal mol^{-1}), the last one also being in equilibrium with **12**, through an *opening-closure* process ($E_{12} - E_{22} \approx 0.9$ kcal mol^{-1}). Finally, a *flipping* process converts **12** into **21** ($E_{12} - E_{21} \approx 0.2$ kcal mol^{-1}). Furthermore, the *opening-closure* process converts isomer **21** into its enantiomeric form. NMR spectra show the complete equivalence of the phenanthroline ligands, indicating the presence in solution of all the isomers, but say nothing about their relative populations. On the basis of such energy differences it may be expected that the isomers are present in solution, at room temperature, in approximately equimolar ratios.

[Pd(H)(phen)$_2$]$^+$ and [Pd(H)(3-tmp-phen)$_2$]$^+$ Complexes

A palladium hydride intermediate, such as [Pd(H)(N–N)(S)]$^+$, where S represents a coordinating solvent molecule, has been proposed to be present in the termination step of the copolymerisation reaction mechanism.[2] Depending upon the reaction conditions, the Pd-hydride can be reoxidised to the catalytically active species, or can insert the olefin starting a new polymeric chain. Eventually, it can evolve to palladium metal. The stability of the active species increases with an excess of the phenanthroline ligand, probably because of the formation of species like [Pd(H)-(phen)$_2$]$^+$, which should prevent the Pd-hydride intermediate from decomposing to palladium metal.[2]

Assuming for this last complex the pseudo-square-pyramidal structure found in the methyl derivatives, MM calculations have been performed for both the phen and the 3-tmp-phen complexes, in order to get some information about their structural behaviour. Inspection of Table 5 shows that, like in the 3-*s*Bu-phen methyl complex, the strain energy slightly increases from isomer **13** to isomer **22**, while **12** and **21** exhibit slightly higher energies. However, the energy trends, as a function of the ligand chirality, are different, and the energy changes are larger.

Table 5. Scaled strain energies [kcal mol^{-1}] for the four diastereoisomers of $[Pd(H)(3\text{-tmp-phen})_2]^+$, all in configuration $\vec{\Delta}$, considering the possible combinations of the ligand chiralities; the torsion angle ψ [°] and the dihedral angle τ [°] are also reported (see footnotes h, i in Table 3).

Isomer	Chirality[a]	ΔE[b]	ψ[b]	τ[b]
13	*S*–*R*	0.0	104.6	74.7
	S–*S*	0.1	105.6	76.4
	R–*S*	1.7	69.8	110.9
	R–*R*	2.0	67.5	111.9
22	*R*–*S*	0.8	–82.3	99.7
	S–*S*	0.9	–71.0	110.2
	R–*R*	1.4	–101.1	79.4
	S–*R*	1.5	–108.2	72.6
12	*S*–*S*	0.9	–69.0	113.5
	S–*R*	1.3	–67.5	113.7
	R–*S*	1.4	–68.6	113.1
	R–*R*	1.8	–68.2	112.6
21	*R*–*S*	1.4	68.7	111.5
	S–*S*	1.4	69.1	110.4
	S–*R*	1.5	74.5	106.9
	R–*R*	1.5	74.0	108.1

[a] The configuration of the asymmetric carbon atoms refers to the tmp-phen group in the chelate and in the monocoordinated phen, respectively. [b] After energy minimisation with a restraint on the Pd···N distance, which results in 2.752 Å.

[Pd{CH(C$_6$H$_5$)CH$_2$C(O)OCH$_3$}(N–N)(L)]$^+$ Complexes

Monocations like [Pd{CH(C$_6$H$_5$)CH$_2$C(O)OCH$_3$}(N–N)(L)]$^+$, where N–N represents chelated phen and 3-tmp-

 © 2005 Wiley-VCH Verlag GmbH & Co. KGaA, Weinheim

phen ligands, and L = CH_3OH or a monocoordinated N–N molecule, are models of possible species involved in the initiation steps of the reaction mechanism for the CO/styrene copolymer chain growth.

In the case of the $[Pd\{CH(C_6H_5)CH_2C(O)OCH_3\}(3\text{-tmp-phen})(CH_3OH)]^+$ derivative, two isomers (*cis* and *trans*) are possible, depending on the relative positions of the growing polymer chain and the nitrogen atom close to the tmp group (Figure 5); while in the case of L = N–N, we have the same isomers of the methyl complexes mentioned above.

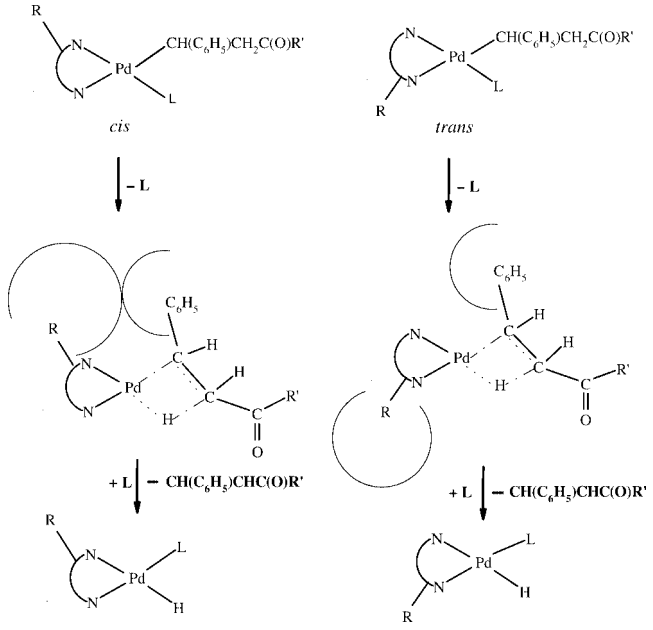

Figure 5. Sketch showing the formation of the transition states for the β-hydrogen elimination process, yielding the termination of the CO/styrene copolymer chain growth; L represents a coordinating solvent or a monocoordinated phen ligand; R′ = OCH_3 or the growing polymer chain; bonds under cleavage or formation are drawn as dotted lines; the arcs depict the steric encumbrance of the R and phenyl groups during their rotation around the C–C bonds.

Examination of molecular models shows that there is no particular difference between the phen and the 3-tmp-phen complexes, as to their steric hindrance to the attack of a further styrene molecule, both in the case of the square-planar (L = CH_3OH) and of the pseudo-square-pyramidal (L = N–N) complexes. Therefore, there is no apparent reason for the observed differences in the copolymerisation reaction, attributable to steric effects in the chain initiation steps.

As a matter of fact, the observation that increasing the bulkiness of the 3-alkyl group remarkably increases the molecular weight of the polymer chains[3] suggests that the bulkiness of the group could play an important role in the chain termination step, which proceeds through a β-hydrogen elimination reaction.[2] As depicted in Figure 5, the reaction intermediate obtained from the *cis* isomer (*cis*-β-H) is destabilised with respect to that obtained from the *trans* isomer (*trans*-β-H) by the steric interactions between the phenyl and the tmp groups, which, at the reaction temperature (≈ 50 °C), can be considered to be freely rotating around their respective single C–C bonds. Because this intermediate leads to the detachment of the copolymer chain, it seems likely that the molecular weight of the copolymer will increase to the extent the β-hydrogen elimination reaction is retarded.

Anyhow, inspection of molecular models (Figure 6, top) indicates that in the *cis*-β-H complex, the repulsive effects are efficient only when the chiral carbon atom of the tmp group and that of the Pd-bound chain exhibit opposite configurations (*R* and *S*, respectively, in Figure 6), displaying the two groups on the same side of the coordination plane. On the contrary, in the case of the *trans*-β-H intermediate (Figure 6, bottom), the two groups are sufficiently distant, even in the case of homochiral groups.

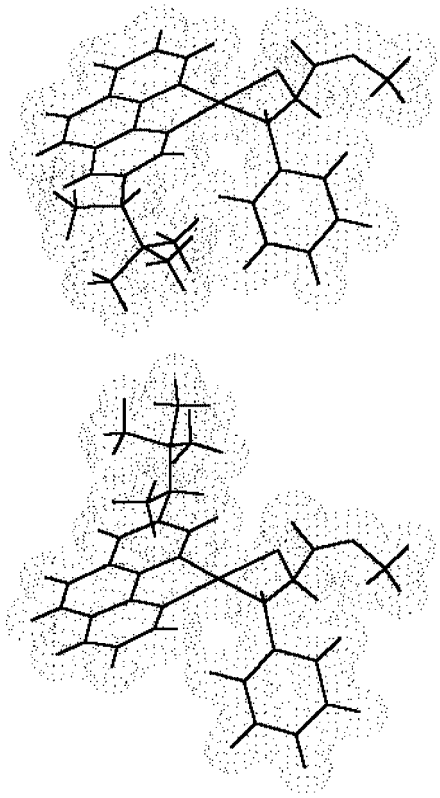

Figure 6. Sketch of the (*R*–*S*)-β-hydrogen elimination intermediate, from the *cis* (top) and *trans* (bottom) isomer of $[Pd\{CH(C_6H_5)CH_2C(O)OCH_3\}(3\text{-tmp-phen})(L)]^+$.

On this basis, it is expected that the termination reaction can occur more easily with the phen complexes rather than with the 3-tmp-phen complexes. In this last case, in fact, the *R*–*S* and *S*–*R* diastereoisomers of the *cis* complex are destabilised by steric interactions, reducing the concentration in solution of the palladium species prone to forming the β-H reaction intermediate.

Conclusions

The stereochemistry of Pd-phenanthroline complexes $[Pd(3\text{-R-phen})_2]^{2+}$ (R = H, alkyl group) has been investi-

 © 2005 Wiley-VCH Verlag GmbH & Co. KGaA, Weinheim

gated in relation with their action as precatalysts in the CO/styrene copolymerisation process.

The results of the MM investigation have shown that the specific force field, derived here, is suitable for a description of the molecular structure of the above dications and of organometallic complexes like $[Pd(CH_3)(3\text{-R-phen})_2]^+$. In the first case, steric effects are shown to determine severe distortions from a square-planar coordination geometry of the metal atom. This can explain the instability of the dications, which in solution of coordinating solvents, undergo dissociation of one chelate ligand and substitution with solvent and/or monocoordinated phen molecules, giving rise to the catalytically active species. In the methyl monocations, the coordination polyhedron results to be intermediate between square planar and square pyramidal, one phenanthroline ligand having one nitrogen atom loosely bound to Pd, in a pseudo apical position. The comparison of the strain energies of all the possible diastereoisomers, together with the results of conformational analyses, account for the possible exchange between the various isomers, in agreement with the fluxional behaviour detected in solution by NMR spectroscopy.

Molecular modelling suggests that peculiar steric effects can be displayed by bulky alkyl groups in 3-R-phen complexes during the termination step of the CO/styrene copolymerisation reaction. In fact, the β-hydrogen elimination reaction appears to be hindered in the presence of a bulky group, such as 1,2,2-trimethylpropyl, allowing the formation of longer copolymer chains.

In order to get a deeper insight into the Pd–N bonding in the square pyramidal methyl derivatives, a quantum chemical investigation appears of interest. Of great importance would also be the quantum chemical investigation of the structure of the intermediate species involved in the β-hydrogen elimination reaction, checking the influence of the phenanthroline side groups. These, in fact, cannot be properly treated by MM methods.

Experimental Section

Materials and Instrumentation: The analytical grade solvents and chemicals (Carlo Erba and Aldrich) were used without further purification for synthetic purposes. The dichloromethane used for the synthesis was purified through distillation over $CaCl_2$ and stored under an inert atmosphere. $[Pd(CH_3COO)_2]$ was a loan from Engelhard Italiana SpA. The 3-*s*Bu-phen, in the racemic form, was prepared by Serafino Gladiali from the University of Sassari. ^1H NMR spectra were recorded at 400 MHz with a JEOL EX 400 spectrometer; the resonances were referenced to the solvent peak versus TMS: $CDCl_3$ at δ = 7.26 ppm.

Synthesis of Complexes: All manipulations were carried out under argon and at room temperature by using Schlenk techniques. Elemental analyses (C, H, N), performed at Dipartimento di Scienze Chimiche (Università di Trieste), were in perfect agreement with the proposed stoichiometry. The compound $[Pd(CH_3)(CH_3CN)(3\text{-}s\text{Bu-phen})][OTf]$ was synthesised as previously reported.[5]

Synthesis of $[Pd(CH_3)(3\text{-}s\text{Bu-phen})_2][OTf]$: *rac*-3-*s*Bu-phen (0.26 mmol) was added to a suspension of $[Pd(CH_3)(CH_3CN)(3\text{-}s\text{Bu-phen})][OTf]$ (0.20 mmol) in chloroform (20 mL) (Pd/3-*s*Bu-phen = 1:1.3) yielding an orange solution. After 10 min, the solution was filtered through fine paper and concentrated under vacuum to induce precipitation of the product as an orange solid. The solid was removed by filtration, washed with diethyl ether and vacuum dried. Yield: 80 %. $C_{34}H_{35}F_3N_4O_3PdS$: calcd. C 54.95, H 4.75, N 7.54; found C 54.6, H 4.71, N 7.60. ^1H NMR ($CDCl_3$): δ = 8.73 (br., 2 H, H^9), 8.69 (br., 2 H, H^2), 8.51 (d, 2 H, H^7), 8.30 (s, 2 H, H^4), 8.02 (s, 4 H, $H^{5,6}$), 7.70 (dd, 2 H, H^8), 0.96 (s, 3 H, CH_3), 0.98 (s, 3 H, CH_3) ppm.

Crystallography: Diffraction data for $[Pd(CH_3)(3\text{-}s\text{Bu-phen})_2][PF_6]\cdot CH_2Cl_2$ were collected at room temperature with the $\omega/2\theta$ scan technique on a CAD4 Enraf–Nonius diffractometer, equipped with graphite-monochromator and Mo-K_α radiation (l = 0.71073 Å). Intensity data were corrected for Lorentz polarisation effects and also for absorption, based on an empirical ψ-scan method. The structure was solved by conventional Patterson and Fourier techniques,[25] and refined by the full-matrix least-squares method based on F^2.[25] The fluorine atoms of the PF_6^- anion were found to be disordered over two positions [refined occupancies of 0.75(2) and 0.25(2)]. A difference Fourier map allowed to detect a disordered molecule of CH_2Cl_2. All the calculations were performed with the WinGX System, Ver 1.64.05.[26] Crystal data: $C_{34}H_{37}Cl_2F_6N_4PPd$, M = 823.95, triclinic, space group $P\bar{1}$ (No. 2), a = 11.002(4), b = 12.508(4), c = 14.502(4) Å, α = 80.67(3), β = 82.37(2), γ = 65.37(3)°, V = 1785.4(10) Å^3, Z = 2, $\rho_{calcd.}$ = 1.533 g cm^{-3}, μ(Mo-K_α) = 0.776 mm^{-1}, F(000) = 836; 7670 reflections collected ($2\theta_{max}$ = 53°), 7367 unique [R(int) = 0.0363], 3332 observed reflections $I > 2\sigma(I)$, 458 parameters, $R1$ = 0.0658, $wR2$ = 0.1658, GoF = 1.017; hydrogen atoms in idealised geometry; max positive and negative peaks in ΔF map 0.561 and –0.637 e Å^{-3}, respectively. CCDC-232498 contains the supplementary crystallographic data for this paper. These data can be obtained free of charge from The Cambridge Crystallographic Data Centre via www.ccdc.cam.ac.uk/data_request/cif.

Acknowledgments

This work was supported by Ministero dell'Istruzione, dell'Università e della Ricerca (MIUR – Rome; PRIN No. 2003033857). Engelhard Italiana is gratefully acknowledged for a generous loan of $[Pd(CH_3COO)_2]$. The authors wish to thank Prof. Serafino Gladiali (University of Sassari) for providing a sample of *rac*-3-*s*Bu-phen.

[1] B. Milani, A. Anzilutti, L. Vicentini, A. Sessanta o Santi, E. Zangrando, S. Geremia, G. Mestroni, *Organometallics* **1997**, *16*, 5064–5075.
[2] B. Milani, G. Corso, G. Mestroni, C. Carfagna, M. Formica, R. Seraglia, *Organometallics* **2000**, *19*, 3435–3441.
[3] B. Milani, A. Scarel, G. Mestroni, S. Gladiali, R. Taras, C. Carfagna, L. Mosca, *Organometallics* **2002**, *21*, 1323–1325.
[4] S. Geremia, L. Randaccio, G. Mestroni, B. Milani, *J. Chem. Soc. Dalton Trans.* **1992**, 2117–2118.
[5] B. Milani, A. Marson, E. Zangrando, G. Mestroni, J. M. Ernsting, C. J. Elsevier, *Inorg. Chim. Acta* **2002**, *327*, 188–201.
[6] B. Milani, G. Corso, E. Zangrando, L. Randaccio, G. Mestroni, *Eur. J. Inorg. Chem.* **1999**, 2085–2093.
[7] P. Wehman, V. E. Kaasjager, W. G. J. De Lange, F. Hartl, P. C. J. Kamer, P. W. N. M. van Leeuwen, J. Fraanje, K. Goubitz, *Organometallics* **1995**, *14*, 3751–3761.
[8] A. Scarel, B. Milani, E. Zangrando, M. Stener, S. Furlan, G. Fronzoni, G. Mestroni, S. Gladiali, C. Carfagna, L. Mosca, *Organometallics* **2004**, *23*, 5593–5606..
[9] W. D. Cornell, P. Cieplak, I. R. Bayly, I. R. Gould, K. M. J. Merz Jr., D. M. Ferguson, D. C. Spellmeyer, T. Fox, J. W. Cald-

 © 2005 Wiley-VCH Verlag GmbH & Co. KGaA, Weinheim

well, P. A. Kollman, *J. Am. Chem. Soc.* **1995**, *117*, 5179–5197.
[10] a) S. Geremia, M. Calligaris, *J. Chem. Soc. Dalton Trans.* **1997**, 1541–1547; b) S. Geremia, L. Vicentini, M. Calligaris, *Inorg. Chem.* **1998** , *37*, 4094–4103.
[11] a) S. Geremia, M. Calligaris, L. Randaccio, *Eur. J. Inorg. Chem.* **1999**, 981–992; b) M. Calligaris, L. Randaccio, *Eur. J. Inorg. Chem.* **2002**, 2920–2927.
[12] *HyperChem*, Hypercube Inc., Waterloo, Ontario, **2000**.
[13] M. Calligaris, GEOM, **2001**, University of Trieste, Trieste, Italy.
[14] R. M. Badger, *J. Chem. Phys.* **1934**, *2*, 128–131.
[15] D. R. Herschbach, V. W. Laurie, *J. Chem. Phys.* **1961**, *35*, 458–463.
[16] T. A. Halgren, *J. Am. Chem. Soc.* **1990**, *112*, 4710–4723.
[17] J. V. Rund, A. C. Hazell, *Acta Crystallogr. Sect. B* **1980**, *36*, 3103–3105.
[18] A. Hazell, A. Mukhopadhyay, *Acta Crystallogr. Sect. B* **1980**, *36*, 1647–1649.
[19] a) G. L. Leigh (Ed.), *Nomenclature of Inorganic Chemistry*, Blackwell, Oxford, **1990**; b) A. von Zelewsky, *Stereochemistry of Coordination Compounds*, Wiley, Chichester, **1995**.
[20] A. Bondi, *J. Phys. Chem.* **1964**, *68*, 441–451.
[21] A. Vedani, D. W. Hutha, *J. Am. Chem. Soc.* **1990**, *112*, 6061–6077.
[22] T. W. Hambley, *Inorg. Chem.* **1998**, *37*, 3767–3774.
[23] J. H. Groen, B. J. de Jong, J.-M. Ernsting, P. W. N. M. van Leeuwen, K. Vrieze, W. J. J. Smeets, A. L. Spek, *J. Organomet. Chem.* **1999**, *573*, 3–13.
[24] T. Damhus, C. E. Schäffer, *Inorg. Chem.* **1983**, *22*, 2406–2412.
[25] G. M. Sheldrick, *SHELX97 Programs for Crystal Structure Analysis (Release 97–2)*, University of Göttingen, Germany, **1998**.
[26] L. J. Farrugia, *J. Appl. Crystallogr.* **1999**, *32*, 837–838.
Received May 27, 2004

 © 2005 Wiley-VCH Verlag GmbH & Co. KGaA, Weinheim